

OBSERVATIONS OF [S III] 18.71 MICRON EMISSION IN GALACTIC H II REGIONS

J. F. MCCARTHY, W. J. FORREST, AND J. R. HOUCK

Center for Radiophysics and Space Research, Cornell University

Received 1978 December 15; accepted 1979 February 12

ABSTRACT

Emission of [S III] 18.71 μm radiation has been detected in the Orion Nebula, M17, NGC 2024, and W51, and an upper limit has been set for Sgr A. The line flux from M17 has been mapped with a resolution of 2'.7. A simple theory for predicting the [S III] flux from radio continuum observations is presented and compared with the data. It is found that Orion and M17 are in satisfactory agreement with the observations, and that NGC 2024 is consistent with a low excitation source behind a reasonable amount of 18 μm dust extinction. In W51 the low observed flux may be explained either by low S^{++} abundance or, more likely, by dust extinction. In Sgr A attenuation by dust is the most plausible explanation.

Subject headings: infrared: sources — infrared: spectra — nebulae: general

I. INTRODUCTION

Infrared fine-structure lines can be used to investigate the properties of the dust and ionized gas of H II regions. If the ionized nebula suffers little visual extinction, as in the Orion Nebula, the observed fluxes from fine-structure lines can be used to determine electron densities, temperatures, and ionic abundances, which in turn can be interpreted to yield information about the exciting star and elemental abundances. On the other hand, in the case of heavily obscured nebulae, such as W51, the attenuation due to dust is not negligible, and the comparison of observed fluxes with predictions based on simple models can be useful in estimating the optical constants of the dust, which at present are poorly known.

In the mid-infrared spectra of galactic H II regions, the 18.71 μm line of [S III] is among the strongest observed. It arises from transitions between the 3P_2 and 3P_1 levels in the split ground state of the S^{++} ion. Collisions with electrons populate these levels, and for low enough densities ($n_e \lesssim 6000 \text{ cm}^{-3}$) emission of 18.71 μm radiation is the dominant de-excitation mechanism. For higher densities, de-excitation due to collisions with other electrons becomes dominant, and the emissivity divided by ionic and electron densities drops off as $1/n_e$. The line's location near the center of the 16–20 μm silicate absorption band makes it an ideal probe of the properties of silicate grains, thought to be a major constituent of interstellar dust. Knowledge of the strength of the 20 μm band would be a further constraint on the chemical composition of the grains and would allow better theoretical models of the spectra of cool stars and H II regions where dust emission is important. Furthermore, since the $\text{S}^+ \rightarrow \text{S}^{++}$ ionization potential (23.3 eV) is close to that of $\text{He}^0 \rightarrow \text{He}^+$ (24.6 eV), comparison with radio recombination line observations can give clues to the ionization structure.

Earlier work has detected [S III] 18.71 μm in the

Orion Nebula (Baluteau *et al.* 1976), in W3A (Moorwood *et al.* 1978), and in G333.6–0.2, NGC 7027, and BD+30°3639 (Greenberg, Dyal, and Geballe 1977). This paper reports on detections of [S III] 18.71 μm in Orion, M17, W51, and NGC 2024, and on an unsuccessful search for line emission in Sgr A. We have also mapped line and continuum emission in M17.

II. OBSERVATIONS AND INSTRUMENTATION

The spectra reported here were obtained over a 3 week period in 1977 September and October, using the NASA Lear Jet 30 cm telescope operating at an altitude of 45,000 feet (13.7 km). The circular beam was 2'.7 in diameter and the chopper throw was 8'.1 in azimuth, except for the M17 map, where the amplitude was increased to 16'.2. Except for the Orion Nebula and M17, the 8'.1 throw was large enough to ensure that the reference beam was in empty sky, and in those two cases the line flux in the reference beam is estimated from radio maps (Schraml and Mezger 1969) to be 10% or less of the flux in the main beam.

Spectra of the subsolar point of the Moon were used to correct for the instrumental response and the transmission of the Earth's atmosphere by assuming that the Moon's intrinsic spectrum was a blackbody of temperature 395 K. The absolute flux calibration was based on observations of Mars and Wright's (1976) model for its brightness temperature at 20 μm . (A recent more detailed model [Christensen 1979] of Mars would lower the calibrated fluxes by 1.17.) The flux calibration was checked by observing VY CMa, the 20 μm flux of which agreed with Morrison and Simon (1973). The uncertainty in this calibration is hard to estimate but may be of order $\pm 10\%$. Night-to-night gain variations were $\pm 10\%$ or less. The wavelength calibration was based on laboratory measurements of water lines and was frequently checked by examining the position of zero order.

During this flight series our limiting source of noise

was guiding inaccuracies. Since our dewar samples several closely spaced wavelengths simultaneously, it was possible to make a correction for this guiding noise. This was performed by assuming that when the grating was in one position the average of the 10 channels should be constant within limits set by the other sources of noise, e.g., sky noise and background fluctuations. When an average fell outside these limits, all contributing channels were multiplied by the correction factor necessary to make the average agree with a predetermined value. In the case of sources at the peak of infrared maps, like W51 and M17 S, this value was the maximum observed, while for sources like M17N and θ^2 Ori, which are on the slopes of much stronger sources, the averages were corrected to agree with the mean of all the averages. Typically these guiding corrections were made to about one-third of the integrations and were of order 10%. They improved the shape of the spectrum, thus aiding in identifying the line. However, these corrections also introduced an additional uncertainty into the absolute flux calibration.

These observations were carried out with a new 10-channel liquid-helium-cooled grating spectrometer. The 10 Si:Sb photoconductor detectors are mounted in the focal plane of the $f/7$ single pass Ebert-Fastie configuration, and together they cover a $5 \mu\text{m}$ band with a FWHM spectral resolution of $0.5 \mu\text{m}$. The entire $16\text{--}30 \mu\text{m}$ region can be sampled at a density of three points per resolution element with a total of only nine grating movements. From observations of VY CMa, the in-flight system NEP at $23 \mu\text{m}$ has been estimated to be $8 \times 10^{-14} \text{ W Hz}^{-1/2}$ in each $0.5 \mu\text{m}$ bandpass, with all the detectors equaling this performance within $\pm 10\%$. By allowing for spectrometer transmission, beam splitter reflectivity, and chopper efficiency, we estimate the in-flight detector NEP to be $1.3 \times 10^{-14} \text{ W Hz}^{-1/2}$ for each detector.

Detector output currents first pass through G118 FET transimpedance amplifiers on the cold spectrometer baseplate, thereby avoiding long high impedance leads which are susceptible to microphonic pickup. The signals are next amplified by operational amplifier (op amp) circuits with several available gain settings and then filtered by low pass filters with 100 Hz roll-off. At this point the 10 channels are also averaged by an op amp summing circuit, and this "sum channel" is synchronously demodulated by a lock-in amplifier and displayed on a strip chart. In the absence of correlated noise, this channel gains a $\sqrt{10}$ improvement in signal-to-noise ratio and can be very useful in finding source peaks. All data channels are fed into an IMSAI 8080 microcomputer where they are sampled by a 16-channel 12 bit analog to digital converter. The synchronous demodulation process is carried out in software, using an INTEL 8080 assembly language program, which normally samples and demodulates 12 channels in 1.56 ms (640 Hz). The phase lags between the chopper reference signal and the detector outputs are the same within $\pm 3^\circ$, and the synchronous demodulation routine will accept a single phase delay of up to 32 ms or 180° , whichever

is smaller. The computer can also step the grating according to an easily modified table in its memory, and the results of all integrations are written onto floppy disks and printed on a small data logger. The observer controls the system by means of sense switches which call master routines, and by using a keyboard to enter alphanumeric data. At all times the program's status is displayed on a television monitor and on the front panel LEDs. On board the Kuiper Airborne Observatory, the entire data-acquisition process is automated, with the IMSAI acting in the role of master computer and using the on-board minicomputers as slaves for real-time data analysis and for nodding the telescope. The data-acquisition program occupies 8K bytes of memory plus an additional 4K bytes for a disk operating system.

III. RESULTS

a) Full Spectra

[S III] $18.71 \mu\text{m}$ emission was detected from three beam positions in the Orion Nebula (Trapezium, KL, and θ^2 Ori), M17 S, M17 N, NGC 2024, and W51. No line emission was seen in Sgr A. Between 17.2 and $20.2 \mu\text{m}$, the spectra were fitted to a quadratic baseline and a Gaussian line profile of $\text{FWHM} = 0.5 \mu\text{m}$ and central wavelength $\lambda_c = 18.71 \mu\text{m}$. The results are plotted in Figure 1 and summarized in Table 1. Where large enough to plot, the errors shown in individual data points are standard deviations of the mean derived from the scatter of separate integrations. The quoted errors on line fluxes derive from the fitting procedure and do not include uncertainties in calibration or gain changes. The relatively high χ^2 values in the Orion and M17 S fits can be attributed to two causes. First, there appear to be small systematic point-to-point variations in the spectra which show up as jitter and scatter and which are not described by the statistical errors. Such scatter might be caused by incomplete cancellation of the instrumental response or by guiding noise. If the statistical error of the spectrum of the Trapezium were increased to 2% of the flux, the χ^2 of the fit would be decreased to a more acceptable 1.05. Second, in these high signal-to-noise spectra the line profile suggests a non-Gaussian shape. No attempt was made to eliminate these effects, since it was felt that the desired quantity, the line flux, was sufficiently well determined.

b) M17 Map

Fourteen positions in M17 were examined for [S III] emission; the line was detected in 12 of them. The positions were separated by $1'.8$ and are roughly oriented along and perpendicular to the axis between M17 S and M17 N. Offsetting was from the star BD $-16^\circ 48' 16''$ by means of an xy stage. The chopper throw during the mapping was $16'.2$, ensuring that the reference beam was completely off the H II region as shown in the radio maps (Schraml and Mezger 1969). The spectra were sampled at a density of one point per resolution element, and due to the lower density the

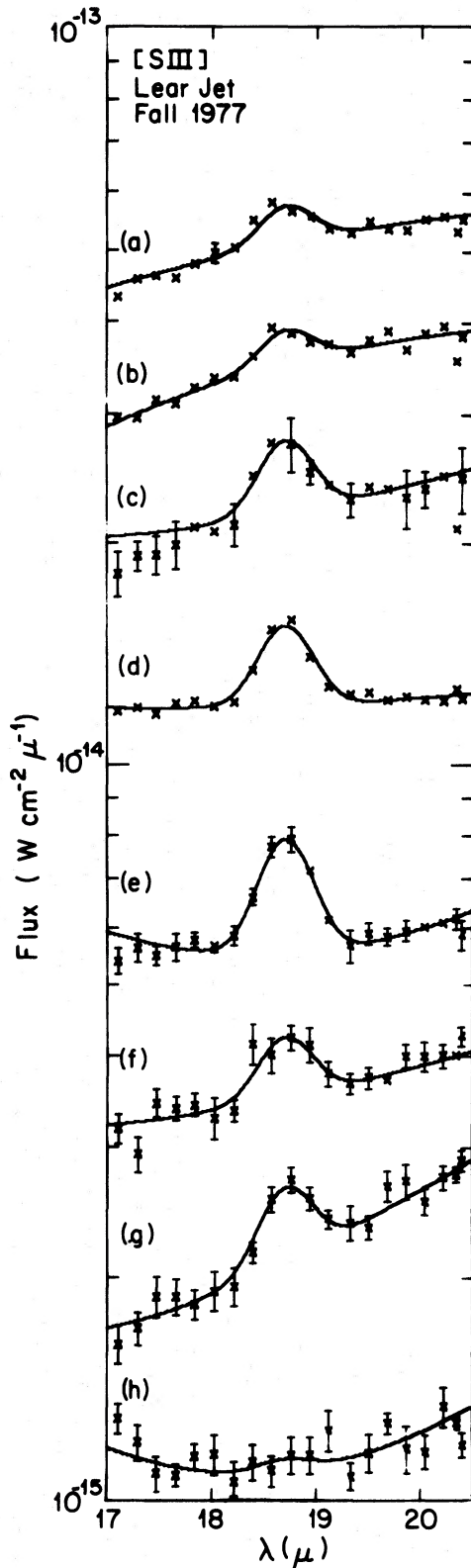
TABLE 1
[S III] 18.71 MICRONS IN H II REGIONS

Object	Galactic Designation	χ^2 per degree of freedom	Fitted Line Flux ($10^{-16} \text{ W cm}^{-2}$)	S_v^* (Jy)	Predicted Line Flux ($10^{-16} \text{ W cm}^{-2}$)	Observed/Predicted	Comments
Trapezium	G209.0-19.4	12.2	23.8±0.8	116	29.3	0.81	
KL			20.1±1.2	81	20.4	0.99	a
θ^2 Ori		2.1	14.1±0.6	66	16.7	0.84	
M17S	G15.0-0.7	3.3	17.2±0.4	91	23.0	0.75	
M17N	G15.1-0.7	0.6	12.0±0.5	66	16.7	0.72	
W51	G49.5-0.4	1.0	3.3±0.6	66	16.7	0.20	
NGC 2024	G206.6-16.4	0.7	3.1±0.3	23	5.8	0.53	
Sgr A		1.2	< 2.3	26	5.8	< 0.40	b

*All fluxes at 15.4 GHz except Sgr A, which is at 5 GHz.

a- The spectrum of KL consists of only a single integration at each wavelength, so no meaningful χ^2 can be calculated. For fitting purposes, $\sigma_\lambda = 0.02F_\lambda$ was assumed, giving $\chi^2 = 1.2$.

b- Value for line flux is a 3σ upper limit.



fitting function was simplified to a linear baseline plus a Gaussian line profile with $\text{FWHM} = 0.5 \mu\text{m}$ and a central wavelength of $18.71 \mu\text{m}$. The results are listed in Table 2 and plotted in Figures 2b and 2c.

IV. CALCULATION OF EXPECTED LINE STRENGTHS

In the absence of extinction, the expression for the [S III] flux from a cloud of ionized gas may be written (Simpson 1975)

$$F = \frac{j}{n_{\text{S III}} n_e} \frac{n_{\text{S III}}}{n_p} \frac{n_p}{n_e} E \Omega,$$

where $(j/n_{\text{S III}} n_e)$ is the emissivity of the ion, $n_{\text{S III}}$, n_e , n_p are the number densities of the S^{++} ions, electrons, and protons, E is the emission measure of the region integrated over the beam, and Ω is the solid angle of the beam.

The emissivity of the ionized gas depends on the electron density and temperature. For $n_e \lesssim 6300 \text{ cm}^{-3}$, collisional de-excitation is negligible, and the emissivity is essentially independent of density and only weakly dependent on temperature (Simpson 1975). Due to collisional de-excitation, the emissivity decreases with increasing n_e for $n_e \gtrsim 6300 \text{ cm}^{-3}$ and falls to half of its low density value at $n_e = 2.5 \times 10^4 \text{ cm}^{-3}$. Observations of Sgr A (Ekers *et al.* 1975; Pauls *et al.* 1976) indicate that collisional de-excitation is negligible in that source. According to Schraml and Mezger (1969), the electron densities of all our other regions are also below 6300 cm^{-3} . However, in at least one case, W51, higher-resolution observations show that most of the radio continuum flux originates from compact, high density sources. On the other hand, high density sources are absent or a small fraction of the total flux in M17 (Matthews, Harten, and Goss 1978; Webster, Altenhoff, and Wink 1971) and in Orion (Webster and Altenhoff 1970). The effects of high density regions on individual sources are considered in more detail below. For the purposes of our simple theory we have assumed $T_e = 10^4 \text{ K}$ and $n_e \lesssim 6300 \text{ cm}^{-3}$ throughout, which gives $(j/n_{\text{S III}} n_e) = 5.2 \times 10^{-22} \text{ ergs cm}^3 \text{ s}^{-1} \text{ sr}^{-1}$.

The abundance of S^{++} was taken to be the average of 12 positions in the Orion Nebula which were measured by Peimbert and Torres-Peimbert (1977) giving $n_{\text{S III}}/n_p = 1.4 \times 10^{-5}$. When corrections for unobserved ionization states (e.g., S IV) are made, it is found that roughly half the sulfur is in S^{++} , most of the rest being S^{+++} . The variations within the nebula are roughly a factor of 2 above and below the mean. For the purposes of this simple theory, we

FIG. 1.—Observed [S III] $18.71 \mu\text{m}$ lines. Sampling is three data points per resolution element, and $\Delta\lambda = 0.5 \mu\text{m}$. The error bars are 1 standard deviation of the mean, and the solid lines are fits to the data. The spectra have been normalized for legibility. Object and normalization factor: (a) Trapezium $\times 1.33$. (b) KL Nebula $\times 1$. (c) θ^2 Orionis $\times 2$. (d) M17 S $\times 1$. (e) M17 N $\times 1$. (f) W51 $\times 1.125$. (g) NGC 2024 $\times 0.9$. (h) Sgr A $\times 0.33$. The curve through the Sgr A data represents the fitted value of the line strength, which is much less than a 3σ detection.

TABLE 2
M17 MAP

#	Position RA(1950)	Dec(1950)	18.7 μ m Continuum		$S_{\nu}(15.4\text{GHz})$ (J_{ν})	Predicted		Comments
			Flux ($10^{-16} \text{ W cm}^{-2} \mu^{-1}$)	Line Flux ($10^{-16} \text{ W cm}^{-2}$)		Line Flux ($10^{-16} \text{ W cm}^{-2}$)	Observed Predicted	
1	18 ^h 17 ^m 32. ^s 7	-16°13'03"	118.8±0.1	20.2±0.5	88	22.3	0.91±0.02	a
2	37. ^s 4	11'40"	49.1±0.7	11.4±1.5	62	15.8	0.72±0.09	
3	42. ^s 1	10'16"	51.7±0.6	14.7±1.1	55	13.9	1.06±0.08	b
4	46. ^s 9	08'52"	24.2±0.7	5.6±1.1	22	5.6	1.00±0.20	
5	28. ^s 0	14'28"	27.3±0.7	4.9±1.0	44	11.1	0.44±0.09	
6	23. ^s 3	15'52"	< 2.3	< 3.0	5.5	1.4	< 2.1	d,e
7	48. ^s 0	11'24"	34.6±0.7	10.3±0.9	48	12.1	0.85±0.07	c
8	53. ^s 8	12'32"	14.8±0.5	5.6±1.4	29	7.4	0.76±0.19	
9	59. ^s 6	13'40"	4.7±0.6	< 9.2	14	3.5	< 1.8	d
10	36. ^s 3	09'08"	48.8±0.9	9.1±1.3	44	11.1	0.82±0.12	
11	30. ^s 5	08'00"	22.9±0.8	5.8±1.4	26	6.5	0.89±0.22	
12	26. ^s 9	11'56"	76.0±0.7	10.6±1.6	51	13.0	0.82±0.12	
13	38. ^s 5	14'12"	72.1±0.7	15.3±2.1	81	20.4	0.75±0.10	
14	44. ^s 4	15'20"	29.2±0.1	7.6±1.3	44	11.1	0.68±0.12	

^a M17 S (Lemke and Low 1972).

^b About 50" to east of M17 N (Lemke and Low 1972), and 80" to east of G15.1-0.7 (Schraml and Mezger 1969).

^c About 50" to west of M17 E (Lemke and Low 1972).

^d Line flux is 3 σ upper limit.

^e Continuum flux is 3 σ upper limit. Beam position is south of M17 S, on fringes of molecular cloud.

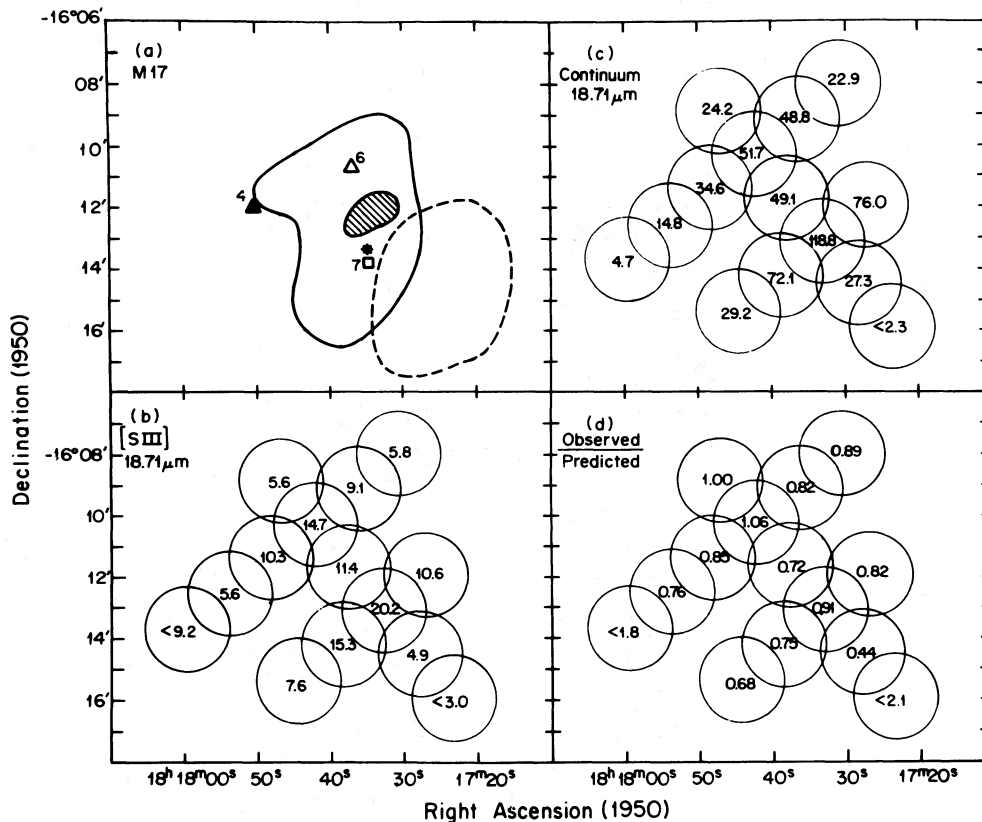


FIG. 2.—(a) Features in the H II region M17. *Asterisk*, the foreground star BD $-16^{\circ}4816$ which was used for offset guiding. *Square* and *open triangle*, positions of radio peaks G15.0–0.7 and G15.1–0.7 (Schraml and Mezger 1969). *Solid line*, half-power contour of 15.4 GHz map, 2' beam (Schraml and Mezger 1969). *Dotted line*, half-power contour of $^{13}\text{C}^{18}\text{O}$ emission (Lada, Dickinson, and Penfield 1974). *Filled triangle*, peak of $\text{H}\alpha$ emission (Dickel 1968). *Hatched ellipse*, center of heavily obscured star cluster (Beetz *et al.* 1976). Numbers give values of A_{ν} to H II region as derived by Dickel (1968) by comparison of radio and $\text{H}\alpha$ fluxes. (b) Map of the integrated [S III] 18.71 μm line flux. Units are $10^{-16} \text{ W cm}^{-2}$, and typical errors are $\pm 1.3 \times 10^{-16} \text{ W cm}^{-2}$. (c) Map of the 18.71 μm continuum. Circles represent the beam positions, and the central numbers give the flux in the 2/7 beam at that position. Units of flux are $10^{-16} \text{ W cm}^{-2} \mu\text{m}^{-1}$, and typical errors (1 standard deviation, derived from the fitting procedure) are $\pm 0.7 \times 10^{-16} \text{ W cm}^{-2} \mu\text{m}^{-1}$. (d) Map of the ratio of the observed [S III] 18.71 μm line flux to that predicted by the theory described in the text. Typical errors in the ratio are ± 0.12 .

have assumed that this abundance is constant for all the regions observed. Finally, the ratio n_e/n_p was taken to be 1.10, since most of the helium should be singly ionized in the region where S^{++} is found.

Except for Sgr A, the emission measure was estimated from the maps of Schraml and Mezger (1969). By assuming that the brightness temperature was constant over the Lear Jet beam, the antenna temperature at the center of the beam was used to calculate the radio flux in the Lear Jet beam. The resulting fluxes are given in Tables 1 and 2. This method overestimates the flux from a point source and underestimates for a source about the size of the radio beam (2'). The error is believed to be no more than a factor of 1.5.

In the case of Sgr A, aperture synthesis observations (Ekers *et al.* 1975) have separated the thermal source, Sgr A West, from the probable supernova remnant, Sgr A East. The integrated flux from Sgr A West is $26 \pm 4 \text{ Jy}$ at 5 GHz, and since the FWHM of the source is only $1' \times <0.6$, all of this flux was included in our Lear Jet beam.

Given the radio flux in the beam, the emission measure can be calculated if a value for T_e is assumed. Under these assumptions, one can then write a simple relation between the [S III] 18.71 μm flux and the optically thin radio free-free continuum, S_{ν} :

$$F(18.71 \mu\text{m}) = 2.04 \times 10^{-16} f(T_e, \nu) (S_{\nu}/1 \text{ Jy}) \text{ W cm}^{-2}$$

where

$$f(T_e, \nu) = (T_e/10^4 \text{ K})^{1/2} [\ln(4.96 \times 10^7 T_e^{3/2} \nu^{-1})]^{-1},$$

and is a slowly varying function of the electron temperature and the radio frequency. For $T_e = 10^4 \text{ K}$ and $\nu = 10 \text{ GHz}$, $f(T_e, \nu) = 0.118$. The total uncertainty due to temperature is small. In the low density limit $T_e = 5000 \text{ K}$ would lower the predicted flux by 5%, while $T_e = 2 \times 10^4 \text{ K}$ would raise it by 10%.

Several of our sources lie behind large column densities of dust, and if this dust contains silicates one can expect attenuation of the [S III] radiation by the 18 μm resonance. Because the strength of the 18 μm feature is uncertain, we have chosen not to include this

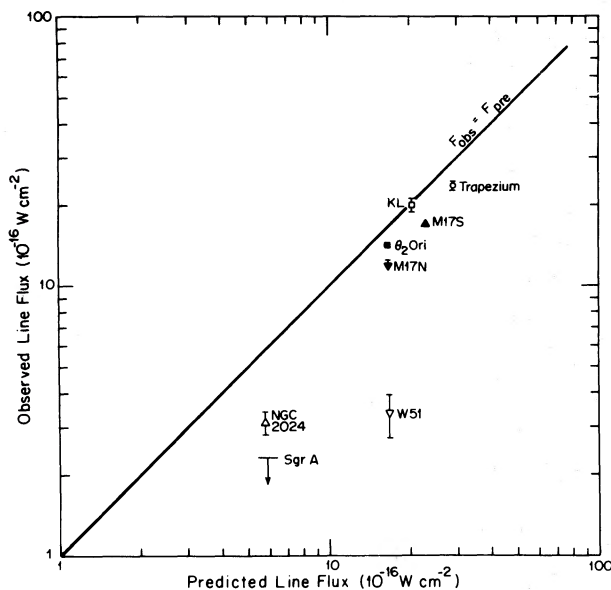


FIG. 3.—Comparison of observed [S III] line flux with that predicted by the simple theory described in the text. Error bars are 1 standard deviation and are derived from the fitting procedure.

extinction in our calculations, but instead to consider the $18\ \mu\text{m}$ optical depth as a quantity which can be measured by comparing the observed flux with that expected in the absence of extinction.

The results of these calculations are given in Tables 1 and 2 and graphed in Figures 2*d* and 3.

V. DISCUSSION

There is a systematic trend for the predicted [S III] fluxes to be too high by an average factor of about 1.3, excluding W51 and observed upper limits. This could be due to one or more of several effects. First, our flux calibration could be low, but the agreement of our spectrum of VY CMa with ground-based measurements argues against this being the major factor. Second, the method of estimating the radio flux may have systematic errors. In order to estimate the magnitude of such errors, models of sources with Gaussian surface-brightness profiles were constructed and the computed fluxes (estimated using the method outlined above) were compared to the exact values. For the source and beam sizes involved, the estimated flux was low by 12% at most, which has the sense of increasing the disagreement. Finally, the assumed ionic abundance may be too high by a factor of 1.3. Given the variations of a factor of 2 in the Orion Nebula (Peimbert and Torres-Peimbert 1977), this seems quite possible.

Orion.—Since the $20\ \mu\text{m}$ silicate feature is seen in emission from the Trapezium (Forrest, Houck, and Reed 1976), the dust optical depth is small, and these observations serve as a useful check on the consistency of the theory. In all three of our beam positions the

agreement between predicted and observed fluxes is good.

Our flux from the Trapezium corresponds to a surface brightness of $(4.9 \pm 0.2) \times 10^{-9}\ \text{W cm}^{-2}\ \text{sr}^{-1}$ averaged over our $2.7''$ beam. This value is a factor of 1.75 times higher than observed by Baluteau *et al.* (1976) (see also Moorwood *et al.* 1978) with a $55''$ beam and does not require a lower value of the sulfur abundance than assumed by Simpson (1975). For a $2.7''$ circular beam centered on the Trapezium, Simpson's model predicts a [S III] flux of $27.4 \times 10^{-16}\ \text{W cm}^{-2}$ (Simpson, private communication), which is also in good agreement with our observations.

M17.—In this source the agreement between predicted and observed fluxes is good. The [S III] flux generally follows the radio flux fairly closely with the possible exception of position 5. Here the beam is at the interface between the H II region and the molecular cloud, so the excitation may be lower or the extinction may be greater. At most of the other points the predicted flux is within 25% of that expected, and the variations are within the errors. There is no strong evidence for systematic changes in the ratio of the predicted to the expected [S III] flux over the nebula.

NGC 2024.—This source appears to have low excitation. The radio recombination lines of He are anomalously weak and the size of the He⁺ source is significantly smaller than that of radio continuum source, as well as being offset by about $1'$ (MacLeod, Doherty, and Higgs 1975). Optical observations (Balick 1976) show that forbidden lines of high ionization species are weak or absent, and that the ratio of He⁺/He integrated over the nebula is less than 0.2. This evidence indicates that the source of the ionizing radiation is cool. Balick models the H II region with $n_e = 10^3\ \text{cm}^{-3}$ and a single star of $T = 33,500\ \text{K}$.

Our predicted flux is approximately twice what is observed, but the interpretation is confused by the presence of substantial dust column densities in the line of sight. Grasdalen (1974) measured $A_v = 8.3 \pm 0.2$ mag toward NGC 2024 No. 1 and $A_v = 32 \pm 6$ toward NGC 2024 No. 2. NGC 2024 No. 1 is on the edge of the dark lane overlying the core of the H II region, so its visual extinction may be used as a lower limit to the mean extinction of the source. We can estimate an upper limit to the $18.71\ \mu\text{m}$ optical depth by assuming that all the sulfur is in S⁺⁺ and that the total sulfur abundance is S/H = 2.6×10^{-5} [log S = 7.41 by number] as given by the average of the positions in Orion (Peimbert and Torres-Peimbert 1977). From this we find $\tau(18.71\ \mu\text{m}) \lesssim 1.3$, which leads to $A_v/\tau(18.71\ \mu\text{m}) \gtrsim 6$. The ratio $A_v/\tau(9.7\ \mu\text{m})$ toward VI Cyg No. 12 is 14 (Gillett *et al.* 1975*b*), and for most silicates the $20\ \mu\text{m}$ resonance is weaker than the $10\ \mu\text{m}$ one, so this lower limit on $A_v/\tau(18.71\ \mu\text{m})$ is entirely reasonable.

Using Balick and Sneden (1976) to derive S⁺⁺/S based on Balick's (1976) model of NGC 2024, one finds that S⁺⁺/S ≈ 0.7 and $\tau(18.71\ \mu\text{m}) \approx 1$. The observed [S III] flux is therefore consistent with the Balick model.

W51.—For this giant H II region, our simple theory predicts 5 times more [S III] flux than observed. At least three effects can be proposed as the cause of this discrepancy: collisional de-excitation in compact regions, low S^{++} abundance, and attenuation by dust.

Much of the radio flux in our beam probably comes from the two compact components seen in the high-resolution radio observations of Martin (1972), Felli, Tofani, and D'Addario (1974), and Scott (1978). These compact H II regions will be referred to by the names given to them by Wynn-Williams, Becklin, and Neugebauer (1974), W51 IRS 1 and W51 IRS 2. In order to estimate the [S III] 18.71 μm line fluxes expected from these sources, the observed radio fluxes have been fitted to a thermal bremsstrahlung model to derive the "optically thin" flux at 5 GHz. This leads to an estimate of approximately 45 ± 10 Jy from W51 IRS 1 and 14 ± 2 Jy for W51 IRS 2. Scott (1978) estimates the electron densities to be $n_e \approx 10^4 \text{ cm}^{-3}$ for W51 IRS 1 and $n_e \approx 2.5 \times 10^4 \text{ cm}^{-3}$ for W51 IRS 2. Then, using the formulation of Petrosian (1970) and Simpson (1975) for the expected strength of the [S III] 18.71 μm line with a S III abundance of 1.4×10^{-5} with respect to protons, the [S III] 18.71 μm line flux should be approximately $8.9 \times 10^{-16} \text{ W cm}^{-2}$ from W51 IRS 1 and $1.7 \times 10^{-16} \text{ W cm}^{-2}$ from W51 IRS 2 or a total of $\sim 10.6 \times 10^{-16} \text{ W cm}^{-2}$ for the compact components alone. The observed line flux of $3.3 \pm 0.6 \times 10^{-16} \text{ W cm}^{-2}$ is approximately a factor of 3 lower than this. Therefore density effects alone are not enough to explain the smaller observed [S III] flux.

Due to the enormous visual obscuration of W51, it is not possible to directly measure the S^{++} abundance as in Orion. Instead one must rely on indirect methods. Based on continuum measurements, Beiging (1975) finds that one or more O4 stars are the exciting stars in these sources. O4 V stars have temperatures of about 50,000 K (Panagia 1973), which is hot enough that about 90% of the sulfur is in S^{+++} (Balick and Sneden 1976). One can next try to observe [S IV] 10.5 μm to check on this. Using Simpson's (1975) emissivity for $T_e = 10^4 \text{ K}$ and $n_e = 10^4 \text{ cm}^{-3}$, a total sulfur abundance of $12 + \log N_s = 7.4$ (Peimbert and Torres-Peimbert 1977), and Martin's emission measure of $72.5 \times 10^6 \text{ pc cm}^{-6}$ and size ($14'' \times 31''$) for IRS 1, we predict F ([S IV] 10.5 μm) = $3.4 \times 10^{-15} f e^{-\tau}$, where $e^{-\tau}$ is the attenuation due to dust and f is the fraction of sulfur in S^{+++} . If we take $f = 1$ and $\tau = 3.9$ (Gillett *et al.* 1975a), we predict F ([S IV] 10.5 μm) = $6.8 \times 10^{-17} \text{ W cm}^{-2}$. Gillett *et al.* (1975a) did not detect [S IV], and an upper limit of about $6 \times 10^{-18} \text{ W cm}^{-2}$ can be set to the line flux. It appears that S^{+++} is less abundant than expected. This is puzzling because [O III] 88 μm is observed at close to the expected strength, assuming an O^{++} abundance like Orion's (Dain *et al.* 1978), but O^{++} and S^{+++} require similar photon energies for their creation. Either S V or S III must be the dominant form. Orion is ionized by $\theta^1 \text{ C Ori}$, which is an O6 or O5 star (Bečvář 1964; Smithsonian Astrophysical Ob-

servatory 1966), so according to Balick and Sneden, $S^{+++}/S > 0.8$ and $S^{++}/S \lesssim 0.05$. Yet the [S III] flux from Orion requires that much of the S be S^{++} , and the [S IV] 10.5 μm line is undetected and weaker than predicted by a factor of 4 (Moorwood *et al.* 1978). By analogy it is plausible that S^{++} is the dominant ion of sulfur in W51 as well. It is unclear why this should be so. Possibilities include (1) the stellar atmosphere models are incorrect; (2) selective ultraviolet extinction by dust cools the radiation field in the H II region; (3) charge exchange reactions are important for sulfur but not for oxygen; and (4) W51 is ionized by a cluster of stars of spectral type later than O4. For a discussion of this point, see Rank *et al.* (1978).

The visual extinction toward W51 IRS 1 and IRS 2 is estimated to be more than 60 and 24 mag, respectively, and both sources show deep 10 μm silicate absorption features (Gillett *et al.* 1975a). Our continuum spectrum shows a shallow 20 μm absorption feature, so large column densities of dust are clearly present. If we assume that the observed flux is lower than expected because of dust extinction, we derive $\tau(18.71 \mu\text{m}) = 1$ or greater, over most of the source.

Sagittarius A.—In this H II region, which is believed to lie at the galactic center, [S III] emission was not detected and a 3σ upper limit of $2.3 \times 10^{-16} \text{ W cm}^{-2}$ may be set, which is a factor of 2.5 below the expected flux. From radio synthesis maps of the thermal component, Sgr A (West), Ekers *et al.* (1975) derived $n_e = 10^3 \text{ cm}^{-3}$, well below the value of 6000 cm^{-3} at which collisional de-excitation begins to lower the emissivity. Plausible arguments that most of the sulfur is in S^{++} may be made from other observations. Mezger and Smith (1976) found that the integrated strength of the He109 α recombination line was 0.095 ± 0.04 times that of H, indicating that almost all He is singly ionized as long as the He abundance is normal. Similarly, observations of [Ne II] 12.8 μm (Aitken *et al.* 1976; Wollman *et al.* 1977) are consistent with most Ne being in Ne^+ , under the assumptions that the Ne abundance is normal and that $\tau(12.8 \mu\text{m}) \approx 1$. On the other hand, [O III] 88 μm radiation is weaker than expected, indicating that O^{++} is underabundant relative to Orion (Dain *et al.* 1978). On the basis of the coincidence of ionization potentials, one can argue that the radiation field is hot enough to make Ne^+ , S^{++} , and He^+ the dominant ions of their elements, but that the ultraviolet flux is not hard enough to create abundant O^{++} or to turn S^{++} into S^{+++} . Therefore we feel our assumption that most of the sulfur is in S^{++} is justified. By elimination, one is left with attenuation by dust for an explanation. The 16–20 μm continuum absorption feature is the deepest one ever seen in our Lear Jet observations, leading one to suspect that extinction is important here. If we interpret the discrepancy between predicted flux and observed upper limit as due solely to dust extinction, then we derive $\tau(18.71 \mu\text{m}) > 0.9$. Further observations with a smaller beam (McCarthy, Forrest, and Houck 1979) allow setting a more stringent limit to the [S III] flux and permit comparison with other wavelengths.

VI. CONCLUSIONS

[S III] 18.71 μm radiation has been detected in the Orion Nebula, M17, NGC 2024, and W51, but not in Sgr A. A simple method of predicting the [S III] flux from the radio continuum flux has been applied, and it has been shown that Orion and M17 agree with the expected flux. The observed line flux in NGC 2024 is consistent with Balick's model for the exciting source, plus a moderate amount of extinction by silicate dust grains. In the case of W51, the low observed flux may be due to either a lower S⁺⁺ abundance than in Orion or dust extinction or both.

The most plausible explanation for the low [S III] emission from the galactic center Sgr A is attenuation by dust.

We would like to thank Robert Mason and the staff of NASA's Airborne Sciences Office for technical support while on the Lear Jet. Gerry Stasavage and Westy Dain receive special thanks for their aid in building the new dewar and the microcomputer system. We are grateful to Dennis Ward, Janet Simpson, and Alan Moorwood for useful conversations. This work was supported by NASA grant NGR 33-010-182.

REFERENCES

- Aitken, D. K., Griffiths, J., Jones, B., and Penman, J. M. 1976, *M.N.R.A.S.*, **174**, 41P.
 Balick, B. 1976, *Ap. J.*, **208**, 75.
 Balick, B., and Sneden, C. 1976, *Ap. J.*, **208**, 336.
 Baluteau, J. P., Bussoletti, E., Anderegg, M., Moorwood, A. F. M., and Coron, N. 1976, *Ap. J. (Letters)*, **210**, L45.
 Bečvář, A. 1964, *Atlas of the Heavens Catalogue* (Cambridge: Sky Publishing House).
 Beetz, M., Elsasser, H., Poulakos, C., and Weinberger, R. 1976, *Astr. Ap.*, **50**, 41.
 Beiging, J. 1975, in *H II Regions and Related Topics*, ed. T. L. Wilson and D. Downes (Berlin: Springer-Verlag), p. 443.
 Christensen, P. 1979, in preparation.
 Dain, F. W., Gull, G. E., Melnick, G., Harwit, M., and Ward, D. B. 1978, *Ap. J. (Letters)*, **221**, L17.
 Dickel, H. R. 1968, *Ap. J.*, **152**, 651.
 Ekers, R. D., Goss, W. M., Schwarz, U. J., Downes, D., and Rogstad, D. H. 1975, *Astr. Ap.*, **43**, 159.
 Felli, M., Tofani, G., and D'Addario, L. R. 1974, *Astr. Ap.*, **31**, 431.
 Forrest, W. J., Houck, J. R., and Reed, R. A. 1976, *Ap. J. (Letters)*, **208**, L133.
 Gillett, F. C., Forrest, W. J., Merrill, K. M., Capps, R. W., and Soifer, B. T. 1975a, *Ap. J.*, **200**, 609.
 Gillett, F. C., Jones, T. W., Merrill, K. M., and Stein, W. A. 1975b, *Astr. Ap.*, **45**, 77.
 Grasdalen, G. L. 1974, *Ap. J.*, **193**, 373.
 Greenberg, L. T., Dyal, P., and Geballe, T. R. 1977, *Ap. J. (Letters)*, **213**, L71.
 Lada, C., Dickinson, D. F., and Penfield, H. 1974, *Ap. J. (Letters)*, **189**, L35.
 Lemke, D., and Low, F. J. 1972, *Ap. J. (Letters)*, **177**, L53.
 MacLeod, J. M., Doherty, L. H., and Higgs, L. A. 1975, *Astr. Ap.*, **42**, 195.
 Martin, A. H. M. 1972, *M.N.R.A.S.*, **157**, 31.
 Matthews, H. E., Harten, R. H., and Goss, W. M. 1978, preprint.
 McCarthy, J. F., Forrest, W. J., and Houck, J. R. 1979, in preparation.
 Mezger, P. G., and Smith, L. F. 1976, *Astr. Ap.*, **47**, 143.
 Moorwood, A. F. M., Baluteau, J. P., Anderegg, M., Coron, N., and Biraud, Y. 1978, *Ap. J.*, **224**, 101.
 Morrison, D., and Simon, T. 1973, *Ap. J.*, **186**, 193.
 Panagia, N. 1973, *A.J.*, **78**, 929.
 Pauls, T., Downes, D., Mezger, P. G., and Churchwell, E. 1976, *Astr. Ap.*, **46**, 407.
 Peimbert, M., and Torres-Peimbert, S. 1977, *M.N.R.A.S.*, **179**, 217.
 Petrosian, V. 1970, *Ap. J.*, **159**, 833.
 Rank, D. M., Dinerstein, H. L., Lester, D. F., Bregman, J. D., Aitken, D. K., and Jones, B. 1978, *M.N.R.A.S.*, **185**, 179.
 Schraml, J., and Mezger, P. G. 1969, *Ap. J.*, **156**, 269.
 Scott, P. F. 1978, *M.N.R.A.S.*, **183**, 435.
 Simpson, J. P. 1975, *Astr. Ap.*, **39**, 43.
 Smithsonian Astrophysical Observatory. 1966, *Star Catalog* (Washington: Smithsonian Institution).
 Webster, W. J., and Altenhoff, W. J. 1970, *Ap. Letters*, **5**, 233.
 Webster, W. J., Altenhoff, W. J., and Wink, J. E. 1971, *A.J.*, **76**, 677.
 Wollman, E. R., Geballe, T. R., Lacy, J. H., Townes, C. H., and Rank, D. M. 1977, *Ap. J. (Letters)*, **218**, L103.
 Wright, E. L. 1976, *Ap. J.*, **210**, 250.
 Wynn-Williams, C. G., Becklin, E. E., and Neugebauer, G. 1974, *Ap. J.*, **187**, 473.

W. J. FORREST, J. R. HOUCK, and J. F. MCCARTHY: Center for Radiophysics and Space Research, Space Sciences Building, Cornell University, Ithaca, NY 14853.